Kinetics and Catalysis, Vol. 46, No. 5, 2005, pp. 719–723. Translated from Kinetika i Kataliz, Vol. 46, No. 5, 2005, pp. 764–768.

Magnetic Methods in a Study of the Effect of the Pore Structure of Silica Gels on the Particle Size of Cobalt in Catalysts for the Fischer–Tropsch Synthesis

G. V. Pankina, P. A. Chernavskii, and V. V. Lunin

Moscow State University, Moscow, 119899 Russia

Received September 24, 2004

Abstract—A magnetic method was proposed for evaluating the average particle size of cobalt metal in supported cobalt catalysts for the Fischer–Tropsch synthesis. This method includes a set of techniques such as *in situ* temperature-programmed reduction and *in situ* temperature-programmed oxidation with simultaneous magnetization measurements and the dependence of magnetization on magnetic field intensity (the field dependence method). It was found that cobalt supported on silica gel with a bimodal pore-size distribution exhibited a special behavior in topochemical processes: the majority of cobalt particles occurred in a superparamagnetic state, while a portion occurred in a multidomain state.

INTRODUCTION

In the past few years, it has been found that the particle size of cobalt in supported cobalt catalysts for the Fischer–Tropsch synthesis is the most important factor responsible for catalytic properties such as activity and selectivity [1–4]. Fu and Bartholomew [1] related this dependence of catalytic properties on the size factor to the structural sensitivity of a catalytic reaction. Evidently, the particle-size distribution of supported cobalt catalysts depends on the pore-size distribution of the supports, in particular, silicates, which are commonly used in the preparation of catalysts for the Fischer–Tropsch synthesis. Thus, Khodakov *et al.* [3] measured the isotherms of low-temperature nitrogen adsorption in a 5% Co/MCM-41 catalyst (MCM-41 is a new class of inorganic silicate oxides with a specified pore size). They found that the pore diameter of the support decreased after impregnation with cobalt nitrate salts, as compared with the initial pore size of the support. The greater the initial diameter, the more significant this decrease.

Characteristically, the pore-size distribution of SiO_2 can be unimodal (i.e., with one maximum in the pore-size distribution curve) or bimodal (i.e., with two maximums corresponding to two different average pore sizes) [5, 6]. Nevertheless, this phenomenon was interpreted as an artifact [3, 7]. The pore structure of the support is responsible for both the degree of reduction and the average particle size of cobalt, which plays the role of an active component [8, 9].

Reliable methods for the *in situ* monitoring of these parameters with a sufficient accuracy are currently unavailable. However, these parameters can be quantitatively evaluated using a magnetic method.

In this work, we used a magnetic method for studying the effect of the pore structure of silica gels on the particle size of cobalt in catalysts for the Fischer–Tropsch synthesis. This method included a set of techniques such as temperature-programmed reduction (TPR) and temperature-programmed oxidation (TPO) with simultaneous *in situ* magnetization measurements and the dependence of magnetization on magnetic field strength (the field-dependence method).

EXPERIMENTAL

The following silica gels were used as supports: S-80; 20% SiO_2 (sol)/S-80; and Q-3, Q-6, and Q-10 CARIACT silica gels (Fujisilysia Chemical) with narrow pore-size distributions. The 20% SiO_2 (sol)/S-80 support with a bimodal pore-size distribution was prepared by impregnating S-80 silica gel (S_{sp} = 80 m^2/g; d_{pore} = 50 nm) with a sol of SiO_2 in a specified concentration [5]. The jelly-like sol of SiO_2 was prepared by the interaction of sodium silicate (20% solution; pH 12.6) with dilute sulfuric acid. Then, the sol was washed with ethanol and hot distilled water to a neutral pH value. After impregnation, the resulting support was dried in air at 80°C for 2 h.

The catalysts were prepared by the triple impregnation of supports with a solution of cobalt nitrate ($Co(NO_3)_2 \cdot 6H_2O$) with a specified concentration followed by drying in air at 80°C for 4 h and calcination at 500°C for 6 h. The Co_3O_4/SiO_2 system with a cobalt concentration of 10 wt % was prepared in this manner.

A flow microreactor of volume 1 ml simultaneously served as a measuring cell of a vibration magnetometer, which allowed us to perform continuous magnetization measurements. The test sample was fixed between two membranes of porous quartz. A thermal conductivity

0023-1584/05/4605-0719 © 2005 MAIK "Nauka/Interperiodica"

Table 1. Characteristics of porous silica gels

Silica gel	S_{sp}, m^2/g	d_{pore}, nm	V_{pore}, cm^3/g	$V_{micropore}$, m^3/g
S-80	70	61.0	0.52	9
20% SiO_2(sol)/S-80	101	30 and 58	–	35
Q-3	550	2.15	0.15	–
Q-6	450	6.25	0.64	–
Q-10	300	~9 and ~11	1.04	–

detector was placed at the reactor outlet. The magnetometer was calibrated before each particular experiment with the use of a high-purity cobalt sample. Magnetization was assumed to be proportional to the weight of cobalt metal. In all of the nonisothermal experiments, the heating rate was 0.3 K/s. The catalyst sample weight was 30 mg.

TPR was performed in a flow of 5 vol % H_2 + Ar. The catalyst was precalcined in a flow of argon at 300°C for 30 min. The reduction process was monitored by measuring the rate of hydrogen consumption. Immediately before oxidation, the catalyst was reduced in hydrogen at 700°C to constant magnetization, which corresponded to a degree of cobalt reduction of about 70%. After reduction, the catalysts were cooled to 7°C in a flow of high-purity argon.

Oxidation was performed in a mixture of 1% O_2 + He under temperature-programmed conditions. Before the onset of TPO, the test sample was oxidized to constant magnetization at 7°C. In this case, an oxide film was formed, which was stable at the specified temperature, and further oxidation was possible only upon increasing temperature.

The coercive force (H_c) and residual magnetization were measured at 7°C. The saturation magnetization σ_s was determined by extrapolation to infinite field in the $1/H - \sigma$ coordinates.

The particle size of cobalt was evaluated after reduction in a flow of H_2 at 500°C. The completeness of reduction was monitored by changes in the magnetization. After reaching a constant value of magnetization, the test sample was cooled to 200°C, and the flow of hydrogen was replaced by argon at the specified temperature in order to desorb H_2 from the surface of cobalt. Next, the temperature was reduced to 7°C (the temperature of water in the reactor cooler). The field dependence of the magnetization of samples at room temperature was measured on a vibration magnetometer with a maximum field of 7.2 kOe. The specific surface areas, average pore sizes, and specific pore and micropore volumes of the supports were measured on a Micrometrics ASAP 2010N instrument.

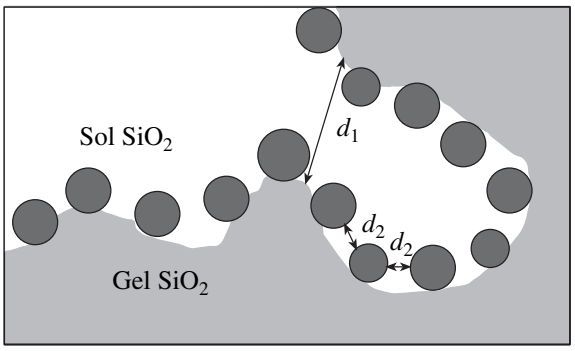

Fig. 1. Schematic diagram of a pore in silica gel with a bimodal size distribution (d_1 and d_2 are diameters).

The X-ray diffraction analysis (DRON-3M) of catalyst samples after oxidation at 300°C demonstrated that the average size of coherent-scattering regions for Co_3O_4 particles was no greater than 15 nm. Thus, the average particle size of cobalt metal in the test systems was smaller than 15 nm.

RESULTS AND DISCUSSION

Table 1 summarizes some characteristics of porous silica gels. As can be seen in Table 1, the S-80, Q-3, and Q-6 supports exhibited unimodal pore-size distributions with average pore sizes of 61.0, 2.15, and 6.25 nm, respectively. The impregnation of the wide-pore S-80 silica gel with a 20% SiO_2 sol resulted in an increase in the specific surface area and the specific pore volume by factors of 1.5 and, on the average, 4, respectively. This suggests the penetration of the sol into the pores of S-80 silica gel and an arbitrary distribution of this sol over the inner walls of the pores [5]. In this case, two types of pores were formed: coarser pores with the average diameter d_1 = 58 nm and smaller pores with the average diameter d_2 = 30 nm. The occurrence of pores with two different average sizes is characteristic of supports with a bimodal pore-size distribution. An analogous pattern was observed in the Q-10 support.

Figure 1 schematically represents a pore of silica gel with a bimodal size distribution, where d_1 and d_2 are the average pore diameters.

Temperature-Programmed Reduction

Previously, it was noted that additional information on the state of a catalyst in the course of its reduction

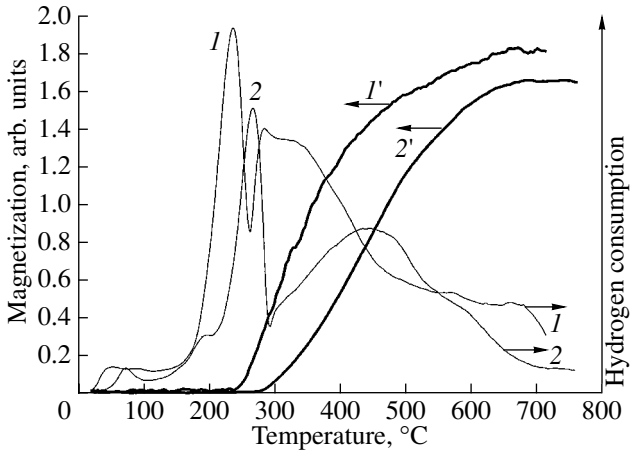

Fig. 2. (*1*, *2*) TPR spectra and (*1*', *2*') the temperature dependence of magnetization for (*1*, *1*') 10% Co/S-80 and (*2*, *2*') 10% Co/20% SiO_2/S-80 catalysts.

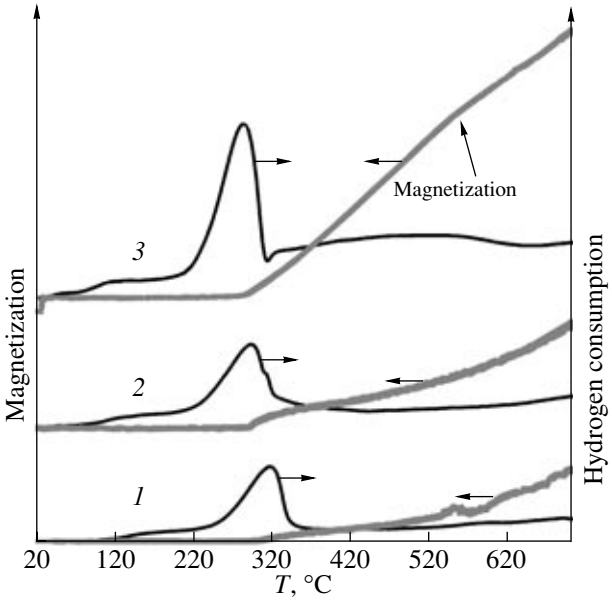

Fig. 3. TPR spectra and the temperature dependence of magnetization for (*1*) 10% Co/Q-3, (*2*) 10% Co/Q-6, and (*3*) 10% Co/Q-10 catalysts.

can be obtained by continuously measuring magnetization in the course of TPR [10]. Because only cobalt metal exhibits ferromagnetic properties in the $Co_3O_4 \longrightarrow CoO \longrightarrow Co$ system, an increase in the magnetization of a sample in the course of TPR is indicative of the reduction of cobalt oxides and the appearance of cobalt metal in the catalyst. Characteristically, the behaviors of cobalt supported on carriers with unimodal and bimodal pore-size distributions in topochemical processes were fundamentally different.

Figure 2 shows the TPR spectra and the temperature dependence of magnetization for 10% Co/S-80 and 10% Co/20% SiO_2 (sol)/S-80 catalysts. Evidently, the first and second TPR peaks correspond to the $Co_3O_4 \longrightarrow Co$ and $CoO \longrightarrow Co$ reduction processes. It can be seen in Fig. 2 that the rate of reduction of the 10% Co/20% SiO_2 (sol)/S-80 catalyst was much lower than that of 10% Co/S-80, and the degree of reduction of the former was lower. This was due to a smaller particle size of cobalt or a higher dispersity of cobalt. Because of this, the oxide–oxide interaction can occur between the active component and the support in this catalyst with the formation of a difficult-to-reduce surface product, cobalt silicate, which is reduced only at elevated temperatures [10]. Moreover, diffusion retardation due to water removal occurred in the system under reduction; this retardation manifested itself particularly strongly in the presence of small cobalt particles. As a rule, small cobalt particles are arranged in the pore channels of the support rather than on the catalyst surface; therefore, H_2O is difficult to remove.

Figure 3 shows the TPR spectra of Co/Q-3, Co/Q-6, and Co/Q-10 catalysts and the corresponding curves for magnetization changes in the course of TPR. It can be seen in Fig. 3 that the rate of reduction decreased as the specific surface area increased and the pore size of the support decreased. The main peak temperature increased from 290°C for Co/Q-10 to 320°C for Co/Q-3.

The amount of hydrogen consumed in the reduction of Co_3O_4 to CoO decreased by a factor of 2 on going from the Co/Q-10 catalyst to the Co/Q-3 catalyst. It is believed that, in the course of reduction, a portion of Co_3O_4 reacted with the silanol groups of silica gel to form a surface silicate, which undergoes reduction only at elevated temperatures [10]. The second fact to be mentioned is the shape of curves that show magnetization changes. The second derivative of magnetization with respect to temperature was positive for the 10% Co/Q-10 catalyst, whereas it was negative for Co/Q-3 and Co/Q-6. In other words, in the case of 10% Co/Q-10, the rate of reduction to metal somewhat decreased with temperature, whereas it continued to increase in 10% Co/Q-3 and 10% Co/Q-6. Note that, although the Q-10 support, which was a constituent of the 10% Co/Q-10 catalyst, exhibited a bimodal pore-size distribution, the catalyst on its basis was reduced much better than the 10% Co/Q-3 and 10% Co/Q-6 catalysts, which exhibited a unimodal pore-size distribution. Evidently, the contribution of coarser cobalt particles to the process of reduction was more significant for the 10% Co/Q-10 catalyst.

It is well known that the particle-size distribution after impregnating a support with cobalt ions can replicate the pore-size distribution of the support, as noted previously [11, 12]. Nevertheless, this is not obvious. This most likely depends on the concentration and temperature of an impregnating solution, the number of impregnation steps, and the conditions of catalyst drying and calcination. This affects the mass transfer and diffusion of metal ions in the interstitial spaces and pore

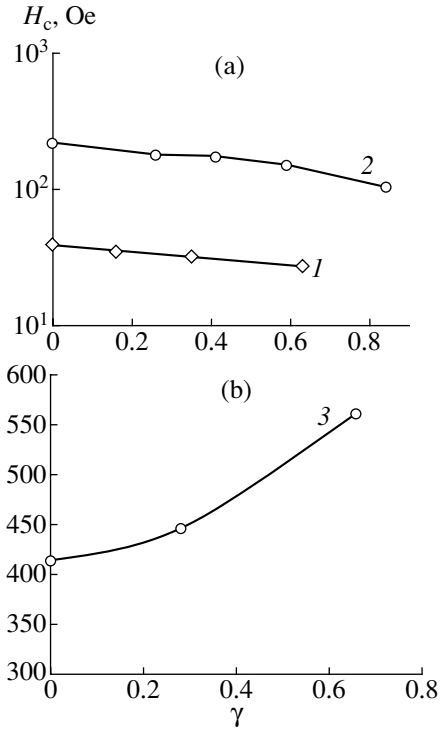

Fig. 4. Dependence of the coercive force (H_c) on the fraction (γ) of oxidized cobalt for (*1*) 10% Co/Q-3, (*2*) 10% Co/Q-6, and (*3*) 10% Co/Q-10 catalysts.

cracks of the support. This problem remains to be solved.

Dependence of Magnetization on Magnetic Field Intensity

To evaluate the boundaries of the particle sizes of cobalt metal, we used the dependence of coercive force (H_c) on the particle size of cobalt, which had the shape of a curve with a maximum [13]. For cobalt, a maximum of H_c corresponded to a size of ~20 nm, which is characteristic of the upper limit of single-domain cobalt particles. This size can be defined as a boundary between small and coarse particles. The coercive force dramatically decreased as the particle size decreased from 20 nm. When the system transformed into a superparamagnetic state, H_c became zero. A multidomain state was characteristic of particles whose size was greater than 20 nm, and H_c also decreased to a limiting value, which corresponded to the state of bulk metal, with particle size.

Table 2. Fraction (γ) of cobalt particles of a given size in supported cobalt catalysts

Catalyst	*d*, nm		
	>10.0	<10.0	>20.0
10%Co/20%SiO_2(sol)/S-80	21	79	–
Co/Q-3	10	90	–
Co/Q-6	30	70	–
Co/Q-10	–	–	≈100

Previously, it was noted that the formation of thin oxide films was observed in the low-temperature oxidation of metals. The kinetics of formation of these films at reduced temperatures can be adequately described by the Cabrer–Mott theory [14]. Evidently, as the oxide film grew as a result of metal oxidation, the maximum size of cobalt particles decreased.

In accordance with the above consideration, the coercive force changes because of the oxidation of cobalt particles (a decrease in the particle size) toward an increase in H_c if the system contains particles greater than 20 nm or toward a decrease in H_c if the system consists of particles smaller than 20 nm.

Figure 4 shows the dependence of H_c on the fraction of oxidized cobalt for Co/Q-3, Co/Q-6, and Co/Q-10, where the amount of cobalt metal after reduction was taken as unity. Note that the coercive force decreased as Co became oxidized in Co/Q-3 and Co/Q-6, whereas it increased in Co/Q-10. Based on the above considerations, we concluded that the Co/Q-3 and Co/Q-6 catalysts did not contain cobalt particles greater than 20 nm. As for the Co/Q-10 catalyst, this system contained particles of sizes greater than 20 nm; that is, all of them belong to a multidomain region.

The ratio of the residual magnetization σ_r to the saturation magnetization σ_s can serve as another important characteristic of the system. The fraction of superparamagnetic particles can be determined from the relation [15]

$$\gamma = 1 - 2\sigma_r/\sigma_s. \quad (1)$$

Because, as demonstrated above, the Co/Q-3 and Co/Q-6 systems did not contain multidomain particles, in this case, the distribution of particles can be analyzed from this standpoint.

In the 10% Co/Q-3 immediately after reduction, 90 wt % Co occurred in a superparamagnetic state at T = 7°C. For the Co/Q-6 system, this value was 70 wt %. The boundary of the particle size of superparamagnetic cobalt can be determined from the condition $KV = 25kT$, where K is the anisotropy constant of cobalt, V is the volume of cobalt particles, k is the Boltzmann constant, and T is the temperature of measurement. We took the anisotropy constant to be 7×10^6 erg/cm^3 [16]. The upper limit of superparamagnetic sizes at room temperature was calculated to be ~10 nm.

Thus, the Co/Q-3 and Co/Q-6 systems mainly contained cobalt particles with superparamagnetic sizes and an insignificant amount of particles with sizes from 10 to 20 nm; the weight fractions of these (single-domain) particles were 10 and 30% for Co/Q-3 and Co/Q-6, respectively. As for the Co/Q-10 system, particles greater than 20 nm, that is, multidomain particles, were present in this system. The presence of these par-

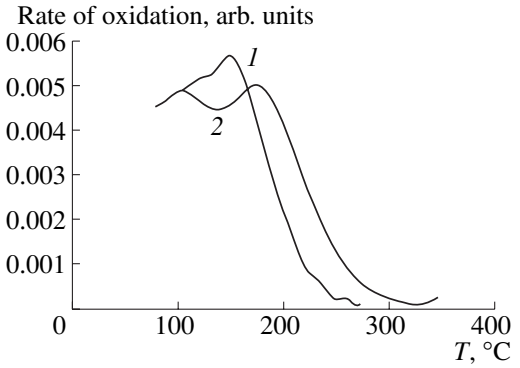

Fig. 5. TPO spectra of (*1*) 10% Co/S-80 and (*2*) 10% Co/20% SiO_2(sol)/S-80 catalysts.

ticles in the system did not allow us to judge correctly the fraction of superparamagnetic particles.

Table 2 summarizes the results of calculations of the weight fraction of superparamagnetic cobalt particles of a certain size (in %) in the test catalysts; these calculations were performed using Eq. (1). It can be seen in Table 2 that the percentage of superparamagnetic particles in the 10% Co/20% SiO_2 (sol)/S-80, 10% Co/Q-3, and 10% Co/Q-6 catalysts was very high, whereas the percentage of nonsuperparamagnetic particles was much smaller. As for the 10% Co/Q-10 catalyst, it is likely that all of the cobalt particles fell in a multidomain region.

Temperature-Programmed Oxidation

The TPO spectra of 10% Co/S-80 and 10% Co/20% SiO_2 (sol)/S-80, which are given in Fig. 5, provide additional information on the particle size of cobalt. Note that the rate of cobalt oxidation was determined from the rate of decrease in magnetization in the $Co_{metal} \longrightarrow CoO$ transition, because Co_3O_4 was not formed at $T = 300$°C, rather than from the rate of oxygen consumption.

Characteristically, the TPO spectra of the 10% Co/20% SiO_2 (sol)/S-80 catalyst exhibited two maximum rates, which correspond to different temperatures and different particle sizes of cobalt metal, whereas the TPO spectrum of 10% Co/S-80 exhibited only a single maximum. As for cobalt supported on the carrier with a bimodal pore-size distribution, smaller particles were initially oxidized at a temperature of 100°C; then, coarser particles were oxidized at a temperature of about ~190°C. It is believed that, because the difference between the peak temperatures was not so great, the difference between the sizes of small and coarse cobalt particles was also not so significant.

This was demonstrated in specially performed experiments on the measurement of the residual magnetization σ_r at the temperatures of maximum points after the TPO process. It was found that the fraction of superparamagnetic particles decreased on going from the first to the second temperature maximum in all of the test systems.

Thus, magnetic methods used for studying supported cobalt catalysts for the hydrogenation of carbon monoxide were found to be highly informative in the evaluation of the average particle size of cobalt metal. Magnetic methods allowed us to distinguish clearly between unimodal and bimodal pore-size distributions.

ACKNOWLEDGMENTS

This work was supported by the Russian Foundation for Basic Research (project no. 02-03-32556).

REFERENCES

1. Fu, L. and Bartholomew, C.H., *J. Catal.*, 1985, vol. 92, p. 376.
2. Jglesia, E., Reyes, S.C., Madon, R.J., and Soled, S.L., *Adv. Catal.*, 1993, vol. 39, p. 221.
3. Khodakov, A.Y., Grihoval-Constant, A., Behara, R., and Zholobenko, V.L., *J. Catal.*, 2002, vol. 206, p. 230.
4. Lapidus, A. and Krylova, A., *Appl. Catal.*, 1992, vol. 80, p. 1.
5. Noritatsu Tsubaki, Yi Zhang, Shouli Sun, Hisashi Mori, Yoshiharu Yoneyama, Xiaohong Li, and Kaoru Fujimoto, *Catal. Commun.*, 2001, vol. 2, p. 311.
6. Pankina, G.V., Chernavskii, P.A., and Lunin, V.V., *Vestn. Mosk. Univ., Ser. 2: Khim.*, 2003, vol. 44, no. 6, p. 372.
7. Gregg, S.J. and Sing, K.S.W., *Adsorption, Surface Area, and Porosity*, New York: Academic, 1982.
8. Chernavskii, P.A., Pankina, G.V., Lermontov, A.S., Torbin, S.N., and Lunin, V.V., *Kinet. Katal.*, 2002, vol. 43, no. 2, p. 292.
9. Chernavskii, P.A., Pankina, G.V., Lermontov, A.S., and Lunin, V.V., *Kinet. Katal.*, 2003, vol. 44, no. 5, p. 718.
10. Chernavskii, P.A. and Lunin, V.V., *Kinet. Katal.*, 1999, vol. 40, no. 3, p. 417.
11. Jacobs, G., Das, T.K., Zhang, Y., Li, J., Recoillet, G., and Davis, B.H., *Appl. Catal., A*, 2003, vol. 233, p. 263.
12. Khodakov, A.Yu., Bechara, R., and Griboval-Constant, A., *Appl. Catal.*, 2002, vol. 254, p. 273.
13. Petrov, Yu.I., *Fizika malykh chastits* (Physics of Small Particles), Moscow: Nauka, 1982.
14. Pankina, G.V., Chernavskii, P.A., and Lunin, V.V., *Zh. Fiz. Khim.* (in press).
15. Weil, L., *J. Chem. Phys.*, 1954, vol. 51, p. 715.
16. Broto, J.M. and Rakoto, H., *Phys. Rev. B.*, 1998, vol. 57, p. 2925.